JOURNAL OF GEOPHYSICAL RESEARCH, VOL. 96, NO. A5, PAGES 7893-7896, MAY 1, 1991

SOLAR CYCLE VARIATIONS IN THE SIZE AND SHAPE OF THE MAGNETOPAUSE

S. P. Petrinec, P. Song, and C. T. Russell

Institute of Geophysics and Planetary Physics, University of California
Los Angeles, California

Abstract. The 10 years of the ISEE 1 and 2 mission covering much of solar cycle 21 and the beginning of solar cycle 22 allow us to study the position, shape, and motion of the magnetopause throughout the course of changing solar activity. We have determined the size and shape of the magnetopause for each observing season using the ISEE 1 and 2 magnetometer data. IMP 8 data were used to monitor the solar wind changes with the solar cycle. During the 1979-1980 season, at solar maximum the solar wind dynamic pressure was at its lowest values, and at solar minimum the solar wind pressure was at its largest values, more than double the value in the 1979-1980 season. During this solar cycle the magnetopause was about 0.5 R_E farther when the interplanetary magnetic field (IMF) was strongly northward than when strongly southward. Both standoff distance values are found to be smaller than the value found by Fairfield [1971]. The standoff distance of the magnetopause for northward IMF is anticorrelated with the solar wind pressure as expected. However, the standoff distance for southward IMF seems relatively insensitive to solar wind dynamic pressure.

Introduction

The location of the magnetopause is of interest because it marks the limit of direct influence of the Earth's magnetic field. The first estimates of the Earth's magnetopause position and shape were described many years ago [Ferraro, 1960; Spreiter and Briggs, 1962; Mead, 1964; Walters, 1964; Fairfield, 1971]. The shape of the dayside magnetopause of the Earth was fitted to different conic sections by Fairfield, using experimental data of magnetopause crossings from a number of satellite missions during the 1960s. The simplest conic section found to give a good fit to the satellite data for the dayside magnetopause is an ellipsoid, with the Earth centered at one focus. The shape can thus be expressed as:

$$r=\frac{r_o(1+\epsilon)}{(1+\epsilon\cos\theta))} \qquad (1)$$

in which r_o is the standoff distance and ϵ is the eccentricity of the ellipsoid (assumed symmetric about the aberrated x axis). As we will show below, ϵ is close to 0.45 for the Earth.

To lowest order, the location of the magnetopause is determined by pressure balance between the solar wind dynamic pressure and the magnetic pressure of the geomagnetic field. Since the field of the Earth is primarily dipolar, $|B|$ falls off with distance as r^3. Equating the magnetic pressure to the solar wind dynamic pressure, we find that the subsolar magnetopause location should vary inversely as the sixth root of the solar wind dynamic pressure, where ρ is the mass density of the solar wind and v is the bulk solar wind velocity.

$$r_o=k(\rho v^2)^{-1/6} \qquad (2)$$

This paper studies the position and shape of the magnetopause, using ISEE 1 and ISEE 2 magnetometer data over a 10-year period. This enables us to study long-term changes in the magnetopause caused, for example, by solar cycle variations in the solar wind, dynamic pressure, or momentum flux. In addition, corresponding annual average solar wind parameters from the IMP 8 spacecraft are used to compare with the annual variation in the location of the magnetopause.

Magnetopause Shape and Position

The ISEE 1 and 2 spacecraft were in low inclination orbits, whose line of apsides varied relative to the direction of the Sun in the course of the year, such that passes through the dayside magnetopause occurred from June to January. This time period is designated as a season. The associated year given in this paper corresponds to the start of the season. These crossings are identified by eye from magnetometer data as a sudden change in the direction and strength of the magnetic field, due to passage of the spacecraft through the magnetopause current layer. The magnetopause boundary is in constant motion, due to the delicate balance between the magnetic pressure from the Earth and the highly variable dynamic pressure of the solar wind, and is also affected by flux transfer associated with reconnection. The velocity of these magnetopause oscillations is usually greater than that of the spacecraft [Berchem and Russell, 1982]. Thus, depending upon the solar wind conditions and the geometry of the spacecraft trajectory with respect to the magnetopause boundary, multiple crossings are observed often.

All of the ISEE spacecraft positions during magnetopause crossings were measured in GSM coordinates and are shown in Figure 1 as a plot of the distance perpendicular to the aberrated Earth-Sun line versus the distance along the aberrated Earth-Sun line. This display assumes cyclindrical symmetry about this line. The position and time of each pass through the magnetopause was determined. For multiple crossings the time of the crossing was the median time between the first and last crossing of the pass, and the corresponding position of the spacecraft at this time was found.

Altogether this data set comprises 1147 separate crossings (passes) [Song et al., 1988]. The crossings were then distinguished by the orientation and/or magnitude and/or a change in the

Paper number 90JA02566.
0148-0227/91/90JA-02566$02.00

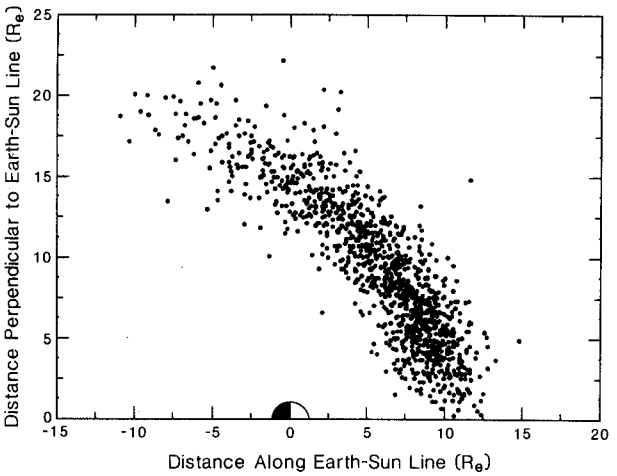

Fig. 1. The location of all magnetopause boundary crossings observed by ISEE from 1977-1987, in GSM coordinates.

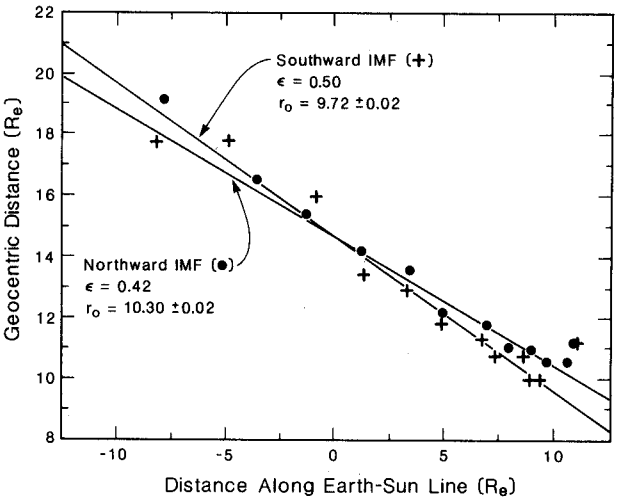

Fig. 2. Plotted medians of r and aberrated x values. The coefficients ϵ and r_o are determined for both northward and southward IMF crossings of the magnetopause.

pattern of magnetic field fluctuations of the interplanetary magnetic field (IMF) as measured by IMP 8, with respect to the magnetic field orientation of the Earth. If IMP 8 was not in the solar wind at the time of the crossing, then ISEE 3 solar wind magnetometer data were used instead. If, however, neither spacecraft was present in the solar wind at the crossing time, then the IMF was inferred from the magnetic field configuration of the magnetosheath. The IMF was divided into three categories; strongly northward, strongly southward, and horizontal. Five-minute IMP 8 magnetic field data (B_y) were charted, with the resulting distribution equi-partitioned into the three separate orientations. When the IMF was more than 26° northward of the GSM equator in the Y-Z plane, it was considered to be strongly northward. Fields more southward than 26° below the equator were considered to be strongly southward. In this study we are only interested in the northward and southward IMF orientations (353 and 364 crossings, respectively), since these configurations represent the extremes in IMF orientation.

For both northward and southward IMF configuration subsets of magnetopause crossings we have determined the median x and r values for angular increments of 10° in the aberrated solar zenith angle θ. We find that the θ bins with the fewest points occur for $0° \leq \theta \leq 10°$ and for $\theta > 110°$ and do not accurately represent the crossings throughout the solar cycle but rather for only a small number of seasons. In addition, the crossings with $\theta > 110°$ have the additional bias imposed by the apogee of the ISEE orbit of 22 R_e such that magnetopause crossings are only seen if the magnetopause is within 22 R_e in this region. The median values as calculated and plotted in Figure 2 have thus been weighted by the number of points in each θ bin from which the median values were found. The best fitting straight line was then determined, using these weighted values, for both IMF orientations and plotted in Figure 2. For northward IMF, crossings give a value for ϵ of 0.42, while for southward IMF we find ϵ = 0.50. The northward IMF crossing set also has a larger standoff distance (r_o = 10.30±0.02 R_e than does that associated with the southward IMF crossing set (r_o = 9.72±0.02 R_e). The values are both significantly smaller than the value of 11.0 R_e found by Fairfield [1971] and by Holzer and Slavin [1978]. The corresponding curves are illustrated in Figure 3. We found that, as expected, the eccentricity of the magnetopause (assuming the ellipsoidal model for the dayside magnetopause) does not change significantly. The difference in standoff distance is understood as due primarily to the increased movement of magnetic flux from the dayside to the nightside when the IMF is southward. Figures 4a and 4b illustrate histograms of the standoff distance for both IMF orientations, showing that for northward IMF, the nose of the magnetopause on average lies a little above 10 R_e, while for southward IMF, this distance is on average less than 10 R_e.

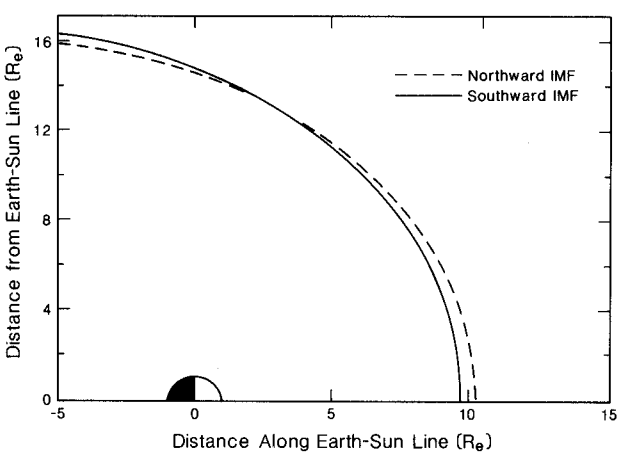

Fig. 3. The characteristic shape of the magnetopause for the calculated ϵ and r_o, for both IMF orientations.

Long-Term Variations

The difference in magnetopause position found in this study from earlier studies suggests that there may be long-term variations in the magnetopause

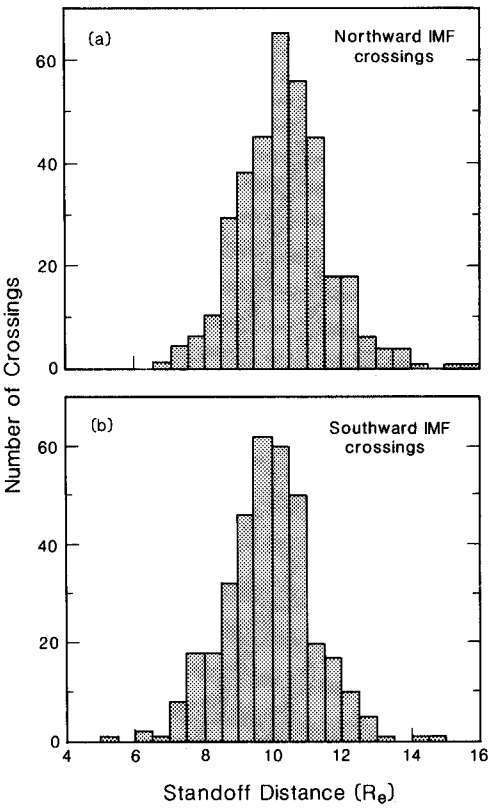

Fig. 4. Histograms of the standoff distance for different IMF conditions (a) Northward IMF configuration. Using 0.5 R_e bins, the most prevalent standoff distance is seen to be slightly above 10 R_e. (b) Southward IMF configuration. The most prevalent standoff distance is seen to be slightly below 10 R_e.

position induced by changes in the solar wind momentum flux. We can check this over the 10 years of the ISEE mission by calculating annual averages of the standoff distance and solar wind parameters. Using IMP 8 data, average solar wind parameters were found for each season, starting 10 days before the first June crossing and continuing until 10 days after the last January crossing (5 min data were used when the IMP 8 spacecraft was in the solar wind).

The standoff distances were divided into three categories, depending upon the IMF. Only northward and southward IMF cases are considered. The average GSM coordinates for each ISEE pass through the magnetopause were used to calculate the corresponding standoff distance using (1), in which we set $\epsilon = 0.42$ for northward IMF, and $\epsilon = 0.50$ for southward IMF. Seasonal averages of the standoff distance were then obtained for both IMF cases. Figure 5 illustrates the average standoff distances for both northward and southward IMF, plotted along with average solar wind dynamic pressure. The error bars signify the error of the mean. The maximum of solar activity (bottom panel) occurs during the 1979-1980 season, when the solar wind dynamic pressure (top panel) is near its minimum, whereas the opposite effect is seen at solar minimum. We observe that the magnetopause standoff distance varies as the solar wind momentum flux varies during the solar cycle. For southward IMF the correlation is weaker but is still present. For northward IMF the correlation coefficient of magnetopause position with solar wind dynamic pressure is 0.70, while for southward IMF the correlation is only 0.43. We consider this lower correlation coefficient for southward IMF to be consistent with our expectation that when the IMF is southward additional processes determine the location of the magnetopause, thus reducing the fraction of the variance "explained" by the change in dynamic pressure.

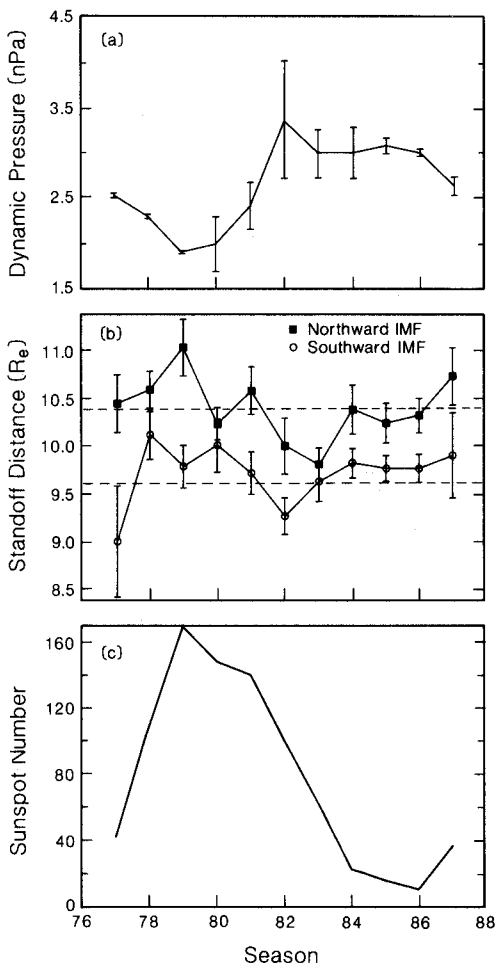

Fig. 5. Changes throughout solar cycle 21 and the beginning of 22. (a) The average solar wind dynamic pressure during the crossing seasons (assumed to consist of 96% Hydrogen and 4% Helium ions). (b) The average standoff distance for each season for both IMF extremes. The error bars reflect the standard error of the mean. The average r_o as determined from this figure is 9.84 ± 0.09 R_e for southward IMF, and 10.37 ± 0.10 R_e for northward IMF, and both are represented by the horizontal dashed lines. (c) The number of sunspots for the same seasons. The maximum of solar activity occurred during the 1979-1980 season, and the minimum occurred during the 1985-1986 season. The average standoff distance is more variable for the northward IMF configuration than for southward IMF orientation throughout this solar cycle and both are inversely correlated to the dynamic pressure.

Discussion

The coefficient k in (2) depends on pressure transmitted by the magnetosheath on the magnetopause and the shape of the magnetopause. Owing to the divergence of stream lines, the full pressure of the solar wind is not transmitted to the magnetopause but rather only about 88% of it [Spreiter et al., 1968]. The dependence of the magnetopause nose position on the shape of the magnetopause can be seen as follows. Consider first the image dipole model of the magnetopause which produces a planar magnetopause [Chapman and Ferraro, 1931]. Inside the magnetopause the field is doubled. Contrast this with the equatorial field of a dipole in a spherical superconductor and the field is tripled. Since the actual shape of the magnetopause lies between a plane perpendicular to the solar wind flow and a sphere (but closer to the latter), we would expect the field enhancement just inside the nose of the magnetosphere to be between 2 and 3. In fact, if we solve for the enhancement factor of the dipole field, we obtain 2.8 for northward IMF and 2.3 for southward IMF, in qualitative agreement with the difference in shape shown in Figure 2. The associated values of k for use in (2) are 0.384 ± 0.005 for northward IMF and 0.365 ± 0.004 for southward IMF.

Conclusions

Using the 10 years of the ISEE 1 and 2 magnetometer data, the size and shape of the magnetopause have been determined for each season, which comprises much of solar cycle 21 and the beginning of solar cycle 22. The magnetopause standoff distance was found to be about 0.5 R_e closer to the Earth for southward IMF than for northward IMF, although there was little change in the associated ellipticity of the boundary. Both values for the average standoff distance were found to be significantly smaller than the value given by Fairfield [1971].

We find the average size of the magnetosphere does vary significantly throughout the course of the solar cycle for both northward and southward IMF orientations. The solar wind dynamic pressure appears to be the dominant factor in the determination of the average standoff position of the magnetopause. The average standoff distances over the solar cycle displayed in Figure 5 are consistent with those obtained from Figure 2. With the solar wind plasma measurements as obtained by IMP 8, we have determined the proportionality constant k between r_o and $(\rho v^2)^{-1/6}$, and assuming that ρv^2 is independent of B_z, it is again observed that when the IMF is northward, the standoff distance of the magnetopause is further from the Earth than when the IMF is oriented southward. The most likely reason for this difference is the transfer of magnetic flux from the dayside magnetosphere to the magnetotail through the reconnection process.

Acknowledgments. This work was supported by the National Aeronautics and Space Administration under research grant NAS5-1067. We are grateful for the NSSDC and H. S. Bridge for the use of the IMP 8 plasma data.

The Editor thanks T. Eastman and another referee for their assistance in evaluating this paper.

References

Berchem, J., and C. T. Russell, The thickness and velocity of the magnetopause current layer: ISEE 1 and 2 observations, J. Geophys. Res., 87, 2108-2114,1982.

Chapman, S., and V. C. A. Ferraro, A new theory of magnetic storms, Terr. Magn., 36, 171, 1931.

Fairfield, D. H., Average and unusual locations of the Earth's magnetopause and bow shock, J. Geophys. Res., 76, 6700, 1971.

Ferraro, V. C. A., An approximate method of estimating the size and shape of the stationary hollow carved out in a neutral ionized stream of corpuscles impinging on the geomagnetic field, J. Geophys. Res., 65, 3951, 1960.

Holzer, R. E., and J. A. Slavin, Magnetic flux transfer associated with expansions and contractions of the dayside magnetosphere, J. Geophys. Res., 83, 3831, 1978.

Mead, G. D., Deformation of the geomagnetic field by the solar wind, J. Geophys. Res., 69, 1181, 1964.

Song, P., R. C. Elphic, and C. T. Russell, ISEE 1 & 2 observations of the oscillating magnetopause, Geophys. Res. Lett., 15, 744, 1988.

Spreiter, J. R., and B. R. Briggs, Theoretical determination of the form of the boundary of the solar corpuscular stream produced by interaction with the magnetic dipole field of the Earth, J. Geophys., Res., 67, 37, 1962.

Spreiter, J. R., A. Y. Alksne, and A. L. Summers, External aerodynamics of the magnetosphere, in Physics of the Magnetosphere, edited by R. L. Carovillano, J. F. McClay, and H. R. Rodoski, p. 301, D. Reidel Publishing Co., Dordrecht-Holland, 1968.

Walters, G. K., Effect of oblique interplanetary magnetic field on shape and behavior of the magnetosphere, J. Geophys. Res., 69, 1769, 1964.

S. Petrinec, C. T. Russell, and P. Song, Institute of Geophysics and Planetary Physics, University of California, Los Angeles, CA 90024.

(Received June 25, 1990;
revised October 22, 1990;
accepted November 20, 1990.)